© OCT 2023 | IRE Journals | Volume 7 Issue 4 | ISSN: 2456-8880
DOI: https://doi.org/10.64388/IREV7I4-1720194

Composition-Driven Atomic Ordering and Glass-Forming Ability of $Fe_{85}Zr_{10}Ni_5$ and $Fe_{88}Zr_{10}Ni_2$ Metallic Glasses: Insights from Molecular Dynamics Simulations

ANIK SHRIVASTAVA
Department of Physics, G.M. Momin Women's College Bhiwandi

Abstract- ***Molecular dynamics simulations are used to investigate the glass forming ability (GFA) and atomic ordering of Fe85Zr10Ni5 and Fe88Zr10Ni2 metallic glass alloys. Structural evolution during fast quenching was studied by means of radial distribution functions and Voronoi tessellation. Both alloys exhibited amorphous features with a strong short range order characterized by distorted icosahedral and Kasper-type polyhedral and reduced glass transition temperature (Trg). Fe85Zr10Ni5 showed higher glass transition temperature Tg = 773K, Trg = 0.571 than Fe88Zr10Ni2 Tg = 752 K, Trg = 0.553, indicating better glass forming ability. The results show that the increase of Ni content improves the local atomic ordering and packing efficiency, thus leading to the improvement of the glass stability. These results provide atomistic insights into the composition-dependent glass formation of Fe-Zr-Ni metallic glasses***

Keywords: molecular dynamics, radial distribution function, metallic glass, kasper-type polyhedral

I. INTRODUCTION

Metallic glasses are a special class of materials, with an atomic structure that is different from that of traditional crystalline alloys. Their lack of long-range atomic periodicity endows them with excellent properties including high strength, excellent corrosion resistance, superior wear resistance, and excellent soft magnetic behavior, which are attractive for structural and functional applications [1,2]. Fe-based metallic glasses are of great interest in the variety of metallic glass systems due to their relatively low cost, high strength, good thermal stability and excellent magnetic properties [3,4]. However, the Fe-based alloys with better glass-forming ability (GFA) are still a great challenge in the development of metallic glasses due to their strong tendency to crystallization during cooling.

Metallic alloys have strong effects on the composition and atomic-scale structure of their glass-forming ability. Small compositional changes may influence atomic packing efficiency, local ordering, thermodynamic stability, and thus affect the formation of an amorphous phase [5]. The addition of Ni to Fe–Zr–Ni alloys is known to change the interatomic interactions and favour the dense packed short-range ordered clusters which prevent the crystallization and favour the glass formation [6,7]. Thus, it is necessary to understand the relationship between composition, atomic ordering and GFA to design Fe-based metallic glasses with improved performance.

Molecular dynamics (MD) simulation is an effective tool to study the structural evolution of metallic glasses at atomic scale [8]. MD allows the simulation of rapid quenching from the liquid state to characterize atomic configurations that are often difficult to probe experimentally. Examples of structural analysis methods providing useful information on short-range order and local atomic environments in amorphous systems include radial distribution functions (RDFs) and Voronoi tessellation [9,10]. In particular, the observation of icosahedral and Kasper-type polyhedra has been correlated with improved glass stability and resistance to crystallization [11].

In the present work, MD simulations were carried out to study the composition-dependent glass formation and atomic ordering in Fe85Zr10Ni5 and Fe88Zr10Ni2 alloys. The glass-forming ability was investigated by the reduced glass transition temperature. The structural origins of glass formation were interpreted using RDF and Voronoi analyses. The results offer atomistic insight into the influence

© OCT 2023 | IRE Journals | Volume 7 Issue 4 | ISSN: 2456-8880
DOI: https://doi.org/10.64388/IREV7I4-1720194

of Ni content on the stability and glass-forming ability of Fe–Zr–Ni metallic glasses.

II. METHOD

The $Fe_{85}Zr_{10}Ni_5$ and $Fe_{88}Zr_{10}Ni_2$ alloys were simulated by the molecular dynamics (MD) in the constant number of particles, pressure and temperature (NPT) ensemble as implemented in the Large-scale Atomic/ Molecular Massively Parallel Simulator (LAMMPS) package [12]. We model the interatomic interactions between Fe, Zr and Ni atoms by using Embedded Atom Method (EAM) potential. The simulation cell consisted of 5000 atoms which were initially placed in a body centered cubic (BCC) lattice and Fe, Zr and Ni atoms were randomly distributed according to the desired alloy compositions. Periodic boundary conditions were applied in the three spatial directions to avoid surface effects and simulate bulk behavior.

The initial structures were equilibrated at 300 K, then heated up to 3000 K, to get a homogeneous liquid. The molten alloys were maintained at 3000 K for 400 ps to ensure a complete melting and to remove any remnant of the initial crystalline arrangement. The liquid alloys were then cooled to 2100 K and quenched to 300 K at cooling rate of $1x10^{11}$ K/s at zero external pressure. The glass transition behavior was determined by monitoring thermodynamic quantities such as volume, enthalpy and density as a function of temperature during coolin

A time step of 2 fs was used during the simulations. The quenched alloys were structurally characterized by radial distribution function (RDF) analysis and Voronoi tessellation to study the short-range atomic ordering and local atomic environments. The glass transition temperature T_g was obtained from the change of the slope of the volume-temperature curve. The glass-forming ability was determined by the reduced glass transition temperature $T_{rg}=T_g/T_m$)) using the Turnbull criterion. All structural and thermodynamic properties were averaged over the last 80 picosecond at each temperature step to ensure statistical reliability.

III. RESULT AND DISCUSSION

Radial Distribution Function (RDF)

Figure 1 shows the radial distribution functions (RDFs) of the $Fe_{85}Zr_{10}Ni_5$ and $Fe_{88}Zr_{10}Ni_2$ alloys in the supercooled state. The RDF profiles of the two compositions are almost identical, suggesting that the overall atomic arrangements are similar despite the different Ni concentrations. A prominent first peak is observed at about 2.4-2.5 Å corresponding to the nearest-neighbor atomic correlations. The sharp and intense character of this peak indicates strong shortrange ordering and efficient packing of atoms in the supercooled liquid. Outside the first coordination shell, the RDF shows damped oscillations of decreasing intensity, characteristic of amorphous materials without long-range periodicity.

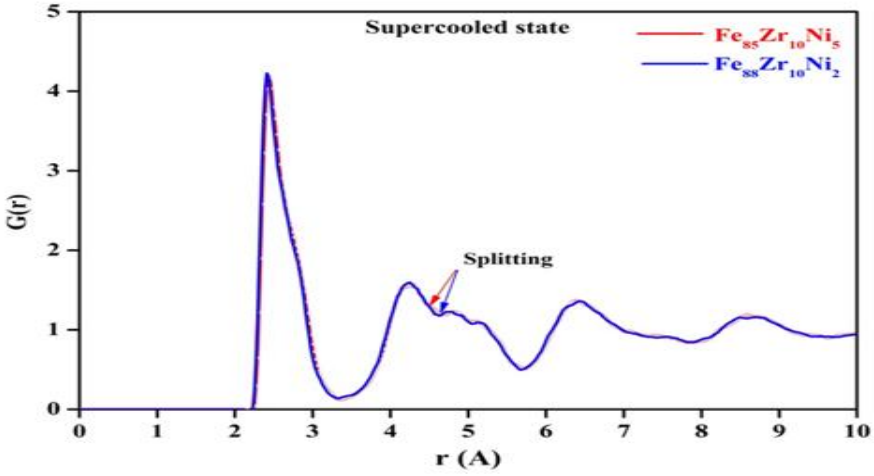

Figure 1. Radial distribution function for $Fe_{85}Zr_{10}Ni_5$ and $Fe_{88}Zr_{10}Ni_2$

© OCT 2023 | IRE Journals | Volume 7 Issue 4 | ISSN: 2456-8880
DOI: https://doi.org/10.64388/IREV7I4-1720194

A prominent feature of the RDF is the splitting of the second peak around 4.5-5.2Å, which is widely accepted as a structural signature of metallic glass formation. This split-second peak indicates the formation of medium range order and presence of local favored atomic clusters during cooling. Such behavior is often associated with densely packed motifs, including distorted icosahedral ones, which increase structural stability and suppress crystallization. The persistence of these split peaks confirms that both alloys have reached a deeply supercooled state with significant amorphous character.

The comparison of the two alloys shows that the Fe85Zr10Ni5 alloy exhibits a more pronounced peak than Fe88Zr10Ni2 that corresponds to a slightly higher degree of local ordering and a slightly more efficient packing of atoms. This is in agreement with the calculated reduced glass transition temperatures, which show that Fe85Zr10Ni5 Trg =0.571 has a higher glass forming ability than Fe88Zr10Ni2 Trg =0.553. The higher Ni content, which causes increased local ordering, probably promotes the formation of stable short-range ordered clusters, thus improving the resistance against crystallization and the glass formation. RDF analysis indicates that both alloys have well developed short and medium range order in the supercooled state, and Fe85Zr10Ni5 has a slightly stronger tendency for glass formation.

Volume-Temperature Curve

The volume–temperature curves obtained during heating and cooling cycles for the $Fe_{85}Zr_{10}Ni_5$ and $Fe_{88}Zr_{10}Ni_2$ alloys are shown in Figure 2(a) and Figure 2(b), respectively. The deflection between the heating and cooling curves is a reflection of the structural changes that occur during melting and solidification and provides useful information about the thermodynamic behavior and glass forming ability of the alloys.

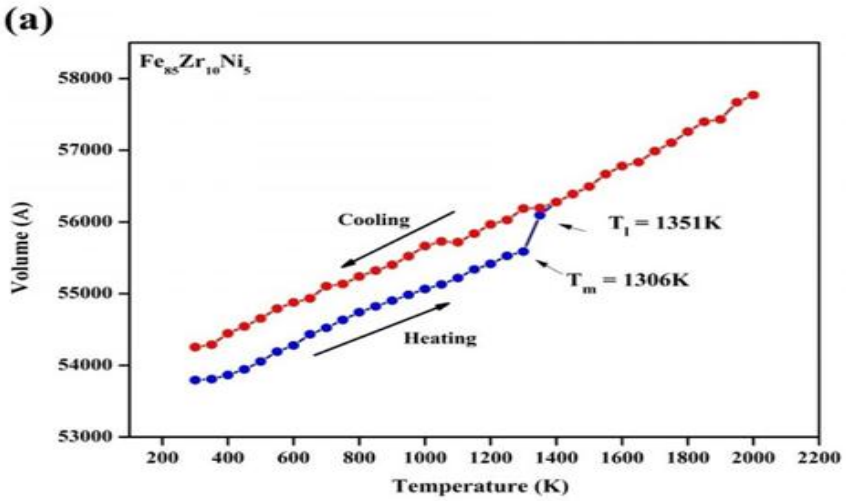

Figure 2 (a) Change in volume as a function of temperature for Fe85Zr10Ni5

For $Fe_{85}Zr_{10}Ni_5$ [Fig. 2(a)], the volume increases nearly linearly with temperature during both heating and cooling. A distinct discontinuity is observed around 1306 K, corresponding to the melting temperature (Tm). During cooling, the liquidus temperature (Tl) is) observed at approximately 1351 K, resulting in a relatively small undercooling interval between melting and solidification. The smooth variation of volume below the liquidus temperature indicates suppression of abrupt crystallization and suggests the formation of a metastable supercooled liquid. The difference between the heating and cooling paths is characteristic of thermal hysteresis associated with amorphous alloy formation.

© OCT 2023 | IRE Journals | Volume 7 Issue 4 | ISSN: 2456-8880
DOI: https://doi.org/10.64388/IREV7I4-1720194

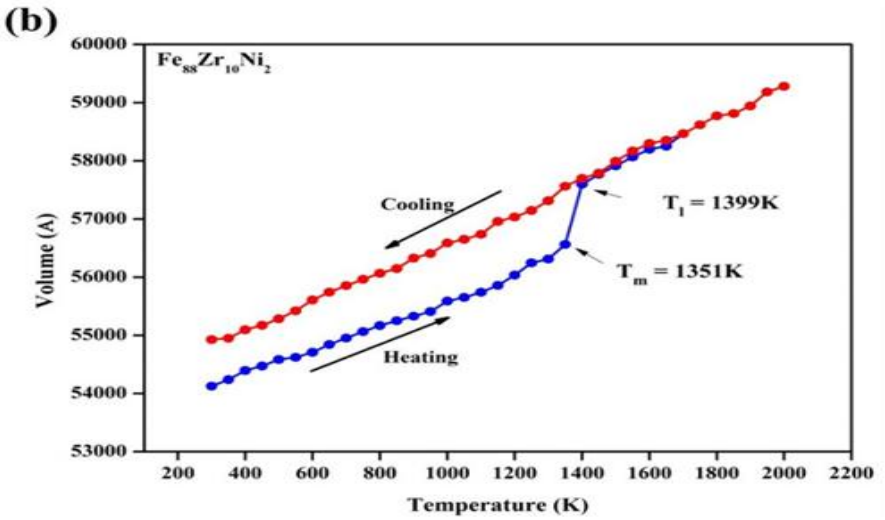

Figure 2 (b) Change in volume as a function of temperature for Fe88Zr10Ni2

Similarly, for $Fe_{88}Zr_{10}Ni_2$ [Fig. 2(b)], the volume exhibits an approximately linear dependence on temperature except in the vicinity of the phase transition region. The melting temperature is determined to be 1351 K, while the liquidus temperature is approximately 1399 K. Compared with $Fe_{85}Zr_{10}Ni_5$, both (Tm) and (Tl) shift to higher temperatures, indicating enhanced thermal stability of the liquid phase. However, the larger separation between the heating and cooling curves suggests a greater tendency toward structural rearrangement during solidification.

The obtained thermodynamic parameters give the reduced glass transition temperature of 0.571 for Fe85Zr10Ni5 and 0.553 for Fe88Zr10Ni2. According to the Turnbull criterion, the higher the reduced glass transition temperature, the better the glass forming ability. Thus, Fe85Zr10Ni5 has better glass-forming ability than Fe88Zr10Ni2, despite the former having lower melting and liquidus temperatures. The enhancement in GFA is ascribed to the increased Ni content that promotes efficient atomic packing and the formation of stable short-range ordered clusters, as evidenced by RDF and Voronoi analyses.

The V-T curves in general indicate that both alloys exhibit typical melting and solidification behavior of amorphous alloys. However, the higher Trg value and lower melting temperature of Fe85Zr10Ni5 show higher crystallization resistance and stronger tendency to keep amorphous structure at rapid cooling, which makes it the better glass former among the two compositions studied

Reduced Glass Transition Temperature (Trg)

The reduced glass transition temperature (Trg=Tg/Tm) is a critical thermodynamic parameter widely used to assess the glass forming ability (GFA) of metallic alloys. In general, according to the Turnbull criterion, the alloys with higher (Trg) values have better resistance to crystallization and are more likely to form an amorphous structure during the rapid cooling process.

Comp (At%)	T_m (K)	T_l (K)	T_g	T_{rg}
$Fe_{85}Zr_{10}Ni_5$	1306	1351	773	0.571
$Fe_{88}Zr_{10}Ni_2$	1351	1399	752	0.533

Table 1. The simulated Tm, Tl, Tg and Trg values for Fe90-XZr10NiX alloys

© OCT 2023 | IRE Journals | Volume 7 Issue 4 | ISSN: 2456-8880
DOI: https://doi.org/10.64388/IREV7I4-1720194

The calculated thermodynamic parameters of the studied alloys are summarized in Table 1. The melting temperature ((Tm)) and glass transition temperature (Tg) was found to be 1306 K and 773 K respectively for Fe85Zr10Ni5 giving a reduced glass transition temperature of (Trg=0.571). On the other hand, Fe88Zr10Ni2 shows a higher melting temperature of 1351 K, but a lower glass transition temperature of 752 K, resulting in a smaller (Trg) value of 0.553.

The Fe85Zr10Ni5 has a higher (Trg) value, indicating that it has a better glass-forming ability than Fe88Zr10Ni2. A larger (Trg) implies that the supercooled liquid region extends closer to the melting temperature, which decreases the thermodynamic driving force for crystallization and promotes glass formation. The increase of Ni content from 2 at.% to 5 at.% seems to enhance the stability of the supercooled liquid by facilitating more efficient atomic packing and formation of stable short range ordered clusters. This interpretation is corroborated by the RDF results indicating a strong split-second peak and by the Voronoi analysis indicating an increased fraction of Fe-centered icosahedral-like polyhedra in $Fe_{85}Zr_{10}Ni_5$.

While the (Trg) values of both alloys are greater than 0.5 indicating good glass-forming tendencies, the highest value of 0.571 obtained for Fe85Zr10Ni5 indicates that this composition has a greater resistance to crystallization during quenching. The $Fe_{85}Zr_{10}Ni_5$ alloy is expected to possess a more stable amorphous structure than $Fe_{88}Zr_{10}Ni_2$.

Local Structure Analysis

Figure 3 illustrates the distribution of dominant Fe-centered and Zr-centered Voronoi polyhedra for $Fe_{88}Zr_{10}Ni_2$ and $Fe_{85}Zr_{10}Ni_5$ metallic glasses. The observed polyhedra represent the most frequently occurring local atomic environments and provide insight into the short-range order responsible for glass formation.

(a)

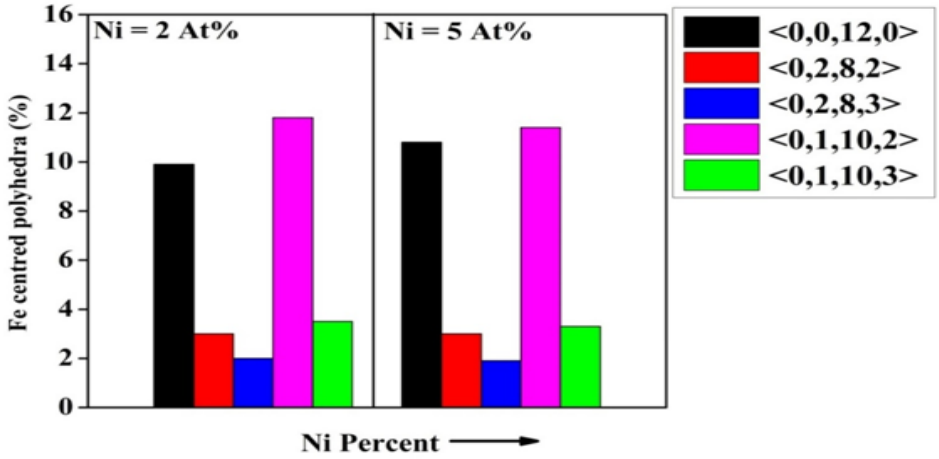

© OCT 2023 | IRE Journals | Volume 7 Issue 4 | ISSN: 2456-8880
DOI: https://doi.org/10.64388/IREV7I4-1720194

(b)

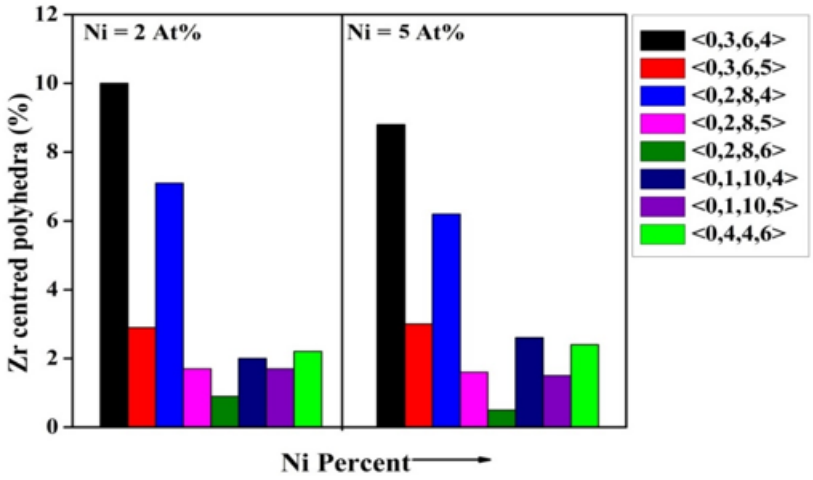

Figure 3 (a) Change in Fe centred polyhedra and (b) Zr centered polyhedral with Nickle percentage

The dominant fractions of Fe-centered polyhedra in both alloys are the clusters of the form ⟨0,0,12,0⟩ and ⟨0,1,10,2⟩, with concentrations larger than 10%. The ⟨0,0,12,0⟩ polyhedron is a perfect icosahedron, a well-accepted highly stable local atomic configuration in metallic glasses. Large fraction of these icosahedral clusters indicates a strong topological ordering and an efficient atomic packing. The fraction of polyhedra of the type ⟨0,0,12,0⟩ increases with increasing Ni concentration from 2 at.% to 5 at.%, whereas the fractions of distorted icosahedral clusters of the types ⟨0,2,8,3⟩ and ⟨0,1,10,3⟩ tend to decrease slightly. The trend suggests that the inclusion of Ni favors local structures that are more stable and more closely packed. The small increase in the ⟨0,1,10,2⟩ population also indicates the enhanced medium-range ordering in the Fe85Zr10Ni5 alloy.

The Zr-centered polyhedra present a more heterogeneous distribution of local environments, mainly represented by the Kasper-type clusters <0,3,6,4> and <0,2,8,4>. The population of the ⟨0,3,6,4⟩ polyhedra decreases from about 10 % in Fe88Zr10Ni2 to about 9 % in Fe85Zr10Ni5. A small reduction of the population of the ⟨0,2,8,4⟩ clusters is also detected. In contrast, polyhedra such as ⟨0,1,10,4⟩ and ⟨0,4,4,6⟩ exhibit a moderate rise with increasing Ni content. These modifications imply a change of the local atomic environment around Zr atoms, leading to a more varied network of close-packed clusters.

The overall, analysis of the Voronoi tessellation reveals that the increase of the Ni content increases the population of the Fe-centered icosahedral-like clusters with a significant fraction of the Zr-centered Kasper-type polyhedra. These local atomic arrangements are known to suppress crystallization by geometric frustration and to increase the packing efficiency. The higher abundance of these stable motifs in Fe85Zr10Ni5 is consistent with its higher reduced glass transition temperature (Trg=0.571)) compared to Fe88Zr10Ni2 (Trg=0.553) confirming the better glass forming ability of the Ni-rich alloy. The results show that the improved GFA of Fe85Zr10Ni5 is attributed to the enhanced formation of icosahedral and Kasper-type SROs that stabilize the amorphous phase and prevent crystallization.

IV. CONCLUSION

We use molecular dynamics simulations to study how the Ni concentration affects the glass forming ability and atomic ordering of Fe85Zr10Ni5 and Fe88Zr10Ni2 metallic glasses. The RDF analysis confirmed the formation of amorphous structures in both alloys by the characteristic splitting of the second peak, while the Voronoi tessellation revealed the predominance of icosahedral-like and Kasper-type polyhedra, indicating stable short-range order.

Thermodynamic analysis showed that $Fe_{85}Zr_{10}Ni_5$ has a higher reduced glass transition temperature (Trg = 0.571) compared with $Fe_{88}Zr_{10}Ni_2$ (Trg = 0.553), indicating a better glass-forming ability. The enhanced GFA is attributed to the increased Ni content resulting in efficient atomic packing, stabilization of the supercooled liquid and suppression of crystallization. These results shed light on the composition-dependent structural evolution of Fe-Zr-Ni metallic glasses at the atomistic level and suggest Fe85Zr10Ni5 as a more promising composition for the development of Fe-based bulk metallic glasses with enhanced structural stability and glass-forming ability.

Acknowledgement
I am thankful to the Naval Material Research Lab (NMRL) and Department of Physics of our college for providing technical support to expand innovative Ideas.

REFERENCES

[1] W. H. Wang, C. Dong, and C. H. Shek, “Bulk metallic glasses,” Mater. Sci. Eng. R 44, 45–89 (2004).

[2] A. Inoue, “Stabilization of metallic supercooled liquid and bulk amorphous alloys,” Acta Mater. 48, 279–306 (2000).

[3] A. L. Greer, “Metallic glasses,” Science 267, 1947–1953 (1995).

[4] J. Schroers, “Processing of bulk metallic glass,” Phys. Today 66, 32–37 (2013).

[5] D. B. Miracle, “A structural model for metallic glasses,” Nat. Mater. 3, 697–702 (2004).

[6] A. Inoue and A. Takeuchi, “Recent development and application products of bulk glassy alloys,” Acta Mater. 59, 2243–2267 (2011).

[7] W. H. Wang, “Roles of minor additions in formation and properties of bulk metallic glasses,” Prog. Mater. Sci. 52, 540–596 (2007).

[8] F. Shimojo, K. Hoshino, and M. Watabe, “Atomic structure and glass formation in metallic liquids studied by molecular dynamics simulation,” Phys. Rev. B 69, 214204 (2004).

[9] D. B. Miracle and P. Harrowell, “Structural aspects of metallic glasses,” Nat. Mater. 16, 45–49 (2017).

[10] H. W. Sheng, W. K. Luo, F. M. Alamgir, J. M. Bai, and E. Ma, “Atomic packing and short-to-medium-range order in metallic glasses,” Nature 439, 419–425 (2006).

[11] J. Saida, A. D. Setyawan, H. Kato, and A. Inoue, “Icosahedral short-range order and glass formation in metallic glasses,” Appl. Phys. Lett. 87, 151907 (2005).

[12] S. Plimpton, "Fast Parallel Algorithms for Short-Range Molecular Dynamics," J. Comput. Phys.117, 1–19 (1995).